Korean J. Chem. Eng., 35(2), 445-455 (2018)
DOI: 10.1007/s11814-017-0296-6

pISSN: 0256-1115
eISSN: 1975-7220

Coal structure change by ionic liquid pretreatment for enhancement of fixed-bed gasification with steam and CO_2

Sang-phil Yoon*,‡, Lingyan Deng,‡, Hueon Namkung***,‡, Shumin Fan*, Tae-Jin Kang*, and Hyung-Taek Kim*,†**

*Department of Energy Systems Research, Ajou University, Woncheon-dong, Youngtong-gu, Suwon 16499, Korea
**Department of Chemical Engineering, McMaster University, Hamilton, Ontario, L8S 4L8, Canada
***Key Laboratory of Coal Gasification and Energy Chemical Engineering of Ministry of Education, East China University of Science and Technology, Shanghai, 200237, P. R. China
(*Received 21 February 2017 • accepted 18 October 2017*)

Abstract−An innovative pretreatment of Indonesian low-rank coal (ILRC) by 1-butyl-3-methylimidazolium chloride ([Bmim]Cl) ionic liquid (IL) was conducted. The obtained IL pretreated coal had a loose and porous structure. Fourier transform infrared spectroscopy (FTIR) and Brunauer-Emmett-Teller (BET) analysis showed that pretreated ILRC had a stronger absorption ability and an increased average pore size (from 23.6 to 51.8 nm). Steam-coal gasification was conducted to explore the effect of coal pretreatment. The result showed that 1.63-times more hydrogen was generated from pretreated coal compared to original (i.e., untreated) coal, and carbon conversion (X_c) increased from 89.03 to 97.25%. During CO_2 coal gasification, IL pretreated coal had a greater CO_2 consumption potential and generated more CO. The chemical exergy of syngas of the pretreated coal gasification was higher than that of the untreated coal gasification with CO_2 at 900 °C. In addition, pretreated coal emitted less CO_2 than untreated coal at 900 °C.

Keywords: Fixed-bed Gasification, Coal Structure, Ionic Liquid Pretreatment, Higher Reactivity

INTRODUCTION

Global warming is becoming an urgent worldwide concern. CO_2 is one of the main greenhouse gases (GHG), most of which is generated by fossil fuel combustion. As one of the three fossil fuels, coal has occupied more than 50% of the world's energy consumption in the past centuries and is going to contribute to power generation in energy sectors. Investment in methods for reducing CO_2 emission is therefore necessary in coal energy systems.

Coal gasification is a key promising technology as the clean coal technology (CCT) to produce versatile energies such as chemicals and electricity [1-4]. One way of reducing CO_2 is using CO_2 as gasification agent and converting it to CO. CO_2 char gasification mostly happens in mesopores, while the steam-char reaction takes place in micropores [5]. The coal pores can be widely separated into three types, based on their size: micropores (pore size, smaller than 2 nm), mesopores (pore size, 2-50 nm) and macropores (pore size, larger than 50 nm) [6-10]. According to Tanner et al. [11], there are three regimes of coal gasification. Regime I is controlled by chemical reaction, regime II by pore diffusion, and regime III by mass transfer. At low temperatures, the rate is controlled by a heterogeneous reaction. While as the temperature increases and approaches the transition to regime II, typically around 1,000 °C, the rate of the chemical reaction increases and delivery of reagent gases to reactive carbon sites by diffusion through the pores begins to influence the overall rate of char conversion. The influence of pore size on chemical reaction rate is increasing at regime II.

A potential method of enhancing CO_2 coal gasification is by changing coal structure, especially by increasing coal pore size, because it has been proved that CO_2 char gasification mostly happens in mesopores [5]. Ionic liquid (IL) pretreatment can change coal pore size and its structure. It can dissolve and swell inorganic and organic structures, such as fibers and polymers [12] and is capable of converting associated hydroxyl groups into dissociated ones. The interaction between coal and ILs results in formation of carboxyl groups. It is widely agreed that low molecular weight compounds and macromolecules coexist in coals, with the former being extractable ILs [13]. It was reported that extraction with 1-butyl-3-methylimidazolium chloride ([Bmim]Cl) significantly changed the type and distribution of hydrogen bonds in Xianfeng lignite coal [14]. [Bmim]Cl is particularly effective in dissolving and swelling lignite coal [15].

Pretreatment of coal with IL to enhance coal liquefaction was well described in previous research, whereas the effect of coal gasification enhancement was not investigated in detail. In this work, an innovative method of IL pretreated coal gasification has been studied. Both steam-coal gasification and CO_2 coal gasification were researched to find the pretreatment effect for the coal particle property and reactivity.

EXPERIMENT AND ANALYSIS

1. Reagents and Apparatus

Indonesian low-rank coal (ILRC) with low sulfur and nitrogen

†To whom correspondence should be addressed.
E-mail: htkim@ajou.ac.kr
‡These authors equally contributed to this work.
‡5th International Conference on Gasification and Its Application.

content was used in this work. Particles of 300-425 μm size were selected by using an appropriate sieve shaker [16]. [Bmim]Cl exhibited optimal performance for coal extraction and lignite swelling, being consistently able to alter the thermal and morphological properties of most coals used [14,15,17-20], and was chosen for this work. [Bmim]Cl with 98% purity was purchased from Sigma-Aldrich. N_2 and CO_2 were purchased from Hanil Gas Inc., with purities of 99.9 and 98 vol%, respectively. Distilled H_2O and CO_2 were used as gasification agents. A furnace was used for both coal pretreatment with [Bmim]Cl and moisture removal.

A high temperature resistant beaker (600 mL volume, 90 mm diameter), used as container for coal pretreatment, was bought from Duran Group. An air filtration pump (Millipore) and a polymer membrane filter (Toyo Roshi Kaisha, Ltd.) with 3.0 μm pore diameter were used to separate IL, residue and pretreated coal. Both pretreated and original coals were subsequently gasified in the same fixed-bed reactor. The fixed-bed reactor, which is 22.5 mm in diameter and 200 mm in height, was constructed in stainless steel with a temperature controller. The reactor was heated using an electric furnace to a predetermined temperature under a stream of nitrogen with a flow rate of 1.5 L/min, controlled through a flow meter. The gasification agents and nitrogen were fed to the top of the fixed-bed reactor, while syngas came out from the bottom, leaving the ash inside the reactor. A detailed description of the fixed-bed reactor can be found in previous study [16]. A continuous online gas analyzer system (i.e., Non-dispersive infrared sensor (NDIR, A&D 9000 Series)) was used to record gas output components.

2. Coal Pretreatment

ILRC and [Bmim]Cl were mixed in a 1 : 10 mass ratio and sealed in a beaker. The mixture was put into a furnace with an optimal temperature of 150 °C [15] and was heated without stirring for 2 h. Subsequently, the mixture was cooled to room temperature. The pretreated coal was washed with distilled water until the washing liquid became colorless and had neutral pH. The collected pretreated coal was dried in a furnace at 70 °C for 48 h to remove surface moisture. Coal structure, pore size, volume, and components could possibly change. A series of analyses were conducted to examine the pretreated and original coal properties.

3. FTIR Analysis

The original coal, pretreated coal and [Bmim]Cl were analyzed by Fourier transform infrared spectroscopy (FTIR) using a single-reflection ATR attachment equipped with a Di crystal. The depth of penetration during the analysis was estimated to be about 2 μm. The spectra were collected using Nicolet iS50/Thermo with 32 scans at 4 cm^{-1} resolution.

4. BET Analysis

According to the IUPAC classification, low-rank coals (C content <75%) mainly contain macropores, coals in the 76-84% fixed carbon range mainly contain micro- and transitional pores, and high-rank coals with >80% fixed carbon mainly contain micropores [8]. Mesopores are accessible to N_2 and CO_2, while micropores are only accessible to CO_2 [6,10]. Standard measurements using CO_2 low pressure gas adsorption techniques can only probe pores with sizes of 0.3-0.85 nm [10], which is in the lower micropore range. Since the coal used herein was low-rank, containing mostly meso- and macropores, N_2 (at 196 °C) was chosen as an adsorptive to characterize the pores of the samples during Brunauer-Emmett-Teller (BET) analysis. N_2 is claimed to cover pores in the range of 1.7-300 nm (higher micro- and the entire mesopore range) [10]. Micromeritics TristarTM 3000 was used as an analytical instrument. Prior to analysis, both coal samples were degassed at atmospheric pressure and 90 °C for 48 h. The adsorption/desorption pressure P/P_0 ranged from 0 to 1.

5. Volumetric Measurements of Coal Samples

Liu et al. [15] measured the swelling ratio by comparing the coal height before and after dissolution in IL. We used a volumetric method to calculate the swelling ratio (Q) of the sample. Original and IL pretreated coal samples (0.6 g each) were placed into a 4 mm inner diameter glass tube. The height of the original and pretreated coal samples was measured and denoted as H_{orig} and H_{pre}, respectively. The swelling ratio was calculated according to the following equation:

$$Q=H_{pre}/H_{orig} \quad (1)$$

6. Coal Gasification

Both original and pretreated ILRC were subjected to gasifying in a fixed-bed reactor. A mixture of 1.5 g of coal and 0.3 g of K_2CO_3 (catalyst) was put into an electrically heated tubular fixed-bed reactor. The experiment was conducted at atmospheric pressure with a temperature range of 700 to 900 °C. Both gasification agents (H_2O/CO_2) and carrier gas (N_2, 1.5 L/min) were preheated at 600 °C and then injected into the top of the reactor. A mixture containing 7.7 vol% of H_2O/CO_2 in N_2 was used in this work. The produced gas exited at the bottom of the reactor and then passed through a cooling system (Lab. Companion RW-0525G) to separate the unreacted steam. The main gas products (H_2, CO, CO_2 and CH_4) were then quantitatively analyzed by NDIR.

7. Evaluation of Thermodynamic Performance During Gasification

The conversion efficiency of coal to syngas can be defined in numerous ways, including feedstock conversion efficiency, syngas yield efficiency, cold gas efficiency and exergy efficiency. Among them, cold gas efficiency (η_c) is considered as an important index for accessing gasifier performance and can be calculated from the following equation:

$$\eta_c=(m_s\times HHV_s)/(m_f\times LHV_f) \quad (2)$$

where m_s and m_f are the mass flow rates of syngas and feed fuels (kg/h), respectively, HHV_s and LHV_f correspond to the high heating value of syngas and the low heating value of feedstock, respectively. The obvious disadvantage of this equation is that it does not consider electrical heating power consumption. The gasification process requires electrical heating to maintain the temperature such as 700, 800, or 900 °C. If consumption of electrical energy is not considered, η_c may exceed 1. Thus, this method is not suitable for our purpose. The exergy efficiency calculation varies among different literatures. Prins et al. [21] defined it as the exergy increase of the gas divided by the exergy decrease of the solid fuel. This definition tends to provide higher efficiencies. Most of the studies use the exergy ratio of the existing products to that of the incoming fuels to represent exergy efficiency [22]. The chemical exergy efficiency is defined as the ratio of the chemical exergy of the product gas to that of input coal [23]. Due to the high temperature condi-

tion for the gasification, physical exergy is also considered. Since CO_2 and N_2 are injected as gasification agent and carrier gas, their physical exergy is counted as input exergy. CO_2 reacts with coal and therefore its chemical exergy should be counted as input exergy. The overall chemical exergy efficiency (η_e) is thus given by:

$$\eta_e=(\Sigma m_s\times(E_S^{ch}+E_S^{ph}))/((m_f\times E_f^{ch})+E^{iph}N_2+E^{iph}CO_2+E^{ich}CO_2) \quad (3)$$

where E_S^{ch}, E_f^{ch} and $E^{ich}CO_2$ denote the chemical exergy of syngas, feedstock coal and input CO_2, respectively, and E_S^{ph}, $E^{iph}N_2$ and $E^{iph}CO_2$ represent the respective physical exergy of syngas, input N_2 and CO_2 from room temperature to the pre-determined gasification temperature.

To determine the chemical exergy of coal, a literature correlation [24] was used:

$$E_f^{ch}=\beta\times LHV \quad (4)$$

$$\beta=\begin{cases}1.0438+(0.0158\times n(H)/n(C))+(0.0813\times n(O)/n(C)), \\ \quad n(O)/n(C)\le 0.5 \\ 1.0414+(0.0177\times n(H)/n(C))-(0.3328\times n(O)/n(C)) \\ \quad \times(1+(0.0537\times n(H)/n(C)))/(0.4021\times n(O)/n(C)), \\ \quad 0.5<n(O)/n(C)\le 2\end{cases} \quad (5)$$

where β is correlation value of chemical exergy of coal, n(H), n(C) and n(O) are mole fractions of the corresponding elements in coal. LHV (=0.943·HHV) is the low heating value of coal and HHV is the high heating value of coal. Two methods for calculating the HHV of fuel exist. One uses the HHV-0 function in the REFSYS correlation property from the Aspen Plus physical property database [25]. The other method uses the correlation developed by Chinniwala and Parikh (in MJ/kg) [26]:

$$HHV_f=(0.3491\times Z_C)+(1.1783\times Z_H)-(0.1034\times Z_O) \\ -(0.0151\times Z_N)+(0.1005\times Z_S)-(0.0211\times Z_A) \quad (6)$$

where HHV_f stands for the high heating value of coal, Z_X (X=C, H, O, N, S and A) represents the weight fraction (dry basis, wt%) of elements and ash (A). This equation was developed for a wide range of fuels, from coal to biomass. In this work, the HHV_f was calculated using Eq. (6).

The physical exergy of a pure substance is given by:

$$E^{ph}=(H-H_0)-(T_0\times(S-S_0))=(H-(T_0\times S))-(H_0-(T_0\times S_0)) \quad (7)$$

where E^{ph} denotes the physical exergy of a pure substance, H and S are the enthalpy and entropy at given temperature and pressure, H_0 and S_0 are the values of the above parameters at standard temperature and pressure (298.15 K, 1 atm) and T_0 is the standard temperature (298.15 K). The values of $H-T_0S$ and $H_0-T_0S_0$ can be conveniently calculated from the Aspen Plus property set using the AVAILMX function.

The chemical exergy of all gaseous components is obtained using the following equation [27]:

$$E^{ch}=\Delta_fG^0+\Sigma n_{el}\times E^{ch}el^0 \quad (8)$$

where E^{ch} is the chemical exergy of gaseous components, Δ_fG^0 denotes the standard Gibbs free energy of formation, n_{el} is the number of moles of the elements in the compound under consideration and $E^{ch}el^0$ is the standard chemical exergy of the elements.

RESULTS AND DISCUSSION

1. Coal Pretreatment

Fig. 1 shows a conceptual diagram of the coal structure changed by pretreatment with [Bmim]Cl. Compared to original coal, the average pore size was increased by a factor of greater than two times, whereas the particle size was slightly decreased. It is obvious that

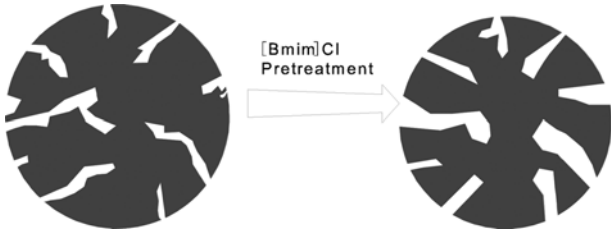

Fig. 1. Conceptual graph of coal structure changes after [Bmim]Cl pretreatment.

Table 1. Proximate and ultimate analysis of original and [Bmim]Cl pretreated coal

		Orig. ILRC	[Bmim]Cl Pre. ILRC
Proximate analysis (air dry basis, wt%)	Moisture	13.63	7.32
	Volatile matter	44.44	49.88
	Fixed carbon	38.63	41.86
	Ash	3.3	0.94
Ultimate analysis (dry basis, wt%)	C	73.11	68.77
	H	3.95	4.90
	O	19.59	22.59
	N	1.02	2.60
	S	0.06	0.13
	Ash	2.27	1.01

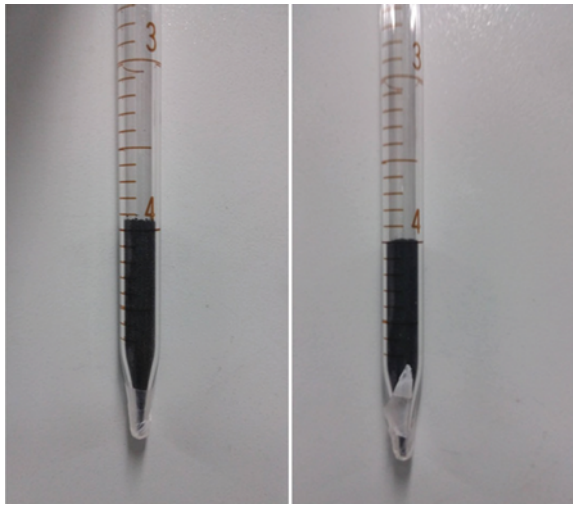

Fig. 2. Volumetric measurement (left: original coal; right: pretreated coal, 0.6 g respectively).

the IL removed a fraction of coal as a result of dissolution and washing with distilled water. Table 1 indicates that coal pretreated with [Bmim]Cl showed a markedly decreased ash content. Nitrogen content clearly increased after pretreatment.

6.00 g of original ILRC yielded about 5.03 g of pretreated ILRC on average. Pretreated coal had a smaller volume than original coal, as shown in Fig. 2, which indicates that pretreatment induces size shrinkage. In this work, original coal had a height of 1.05 cm (H_{orig}), while pretreated coal had a height of 1.0 cm (H_{pre}) on the basis of the same weight.

$$Q=H_{pre}/H_{orig}=0.95 \quad (9)$$

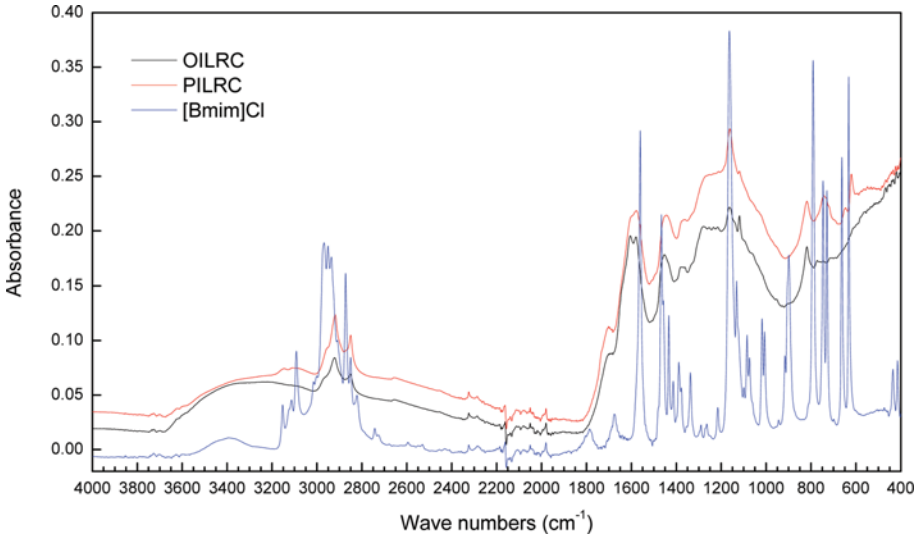

Fig. 3. FTIR spectrum of pretreated coal, original coal and [Bmim]Cl (OILRC: original ILRC, PILRC: pretreated ILRC).

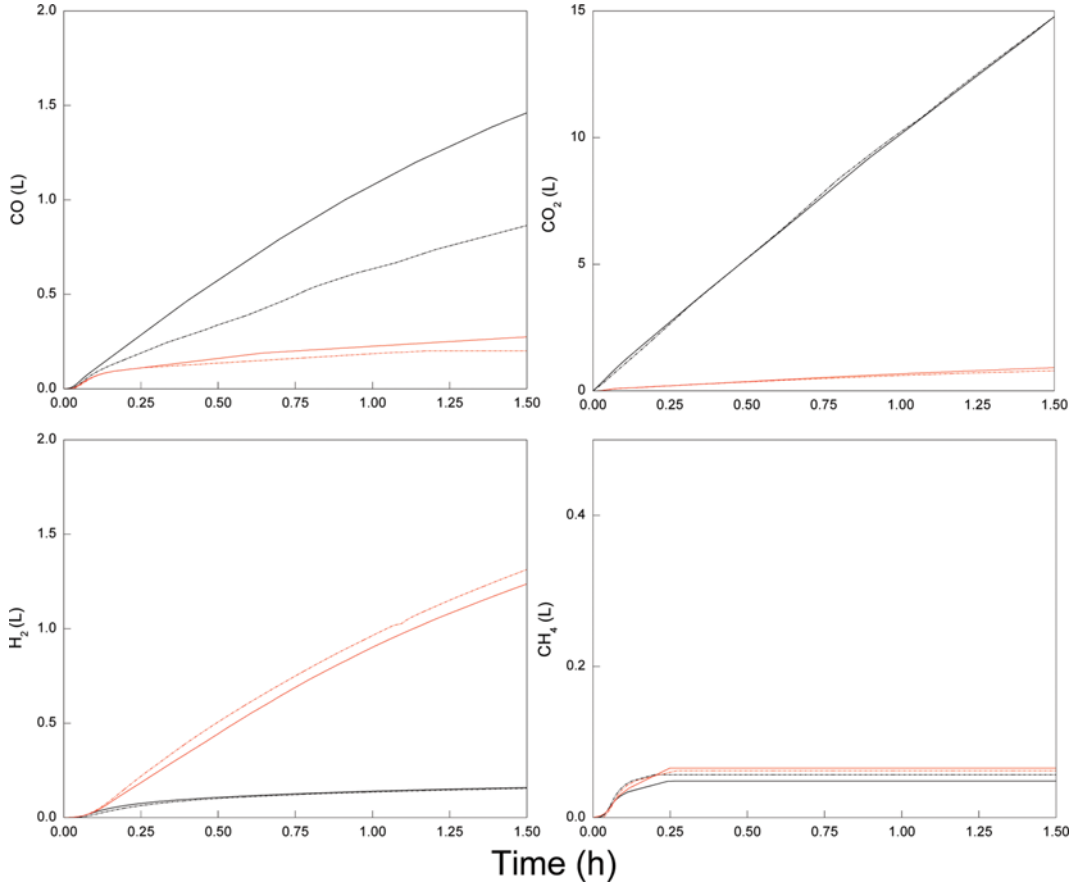

Fig. 4. Main products of coal gasification at 700 °C (red: using H_2O; black: using CO_2, Solid line: original coal; dotted line: pretreated coal).

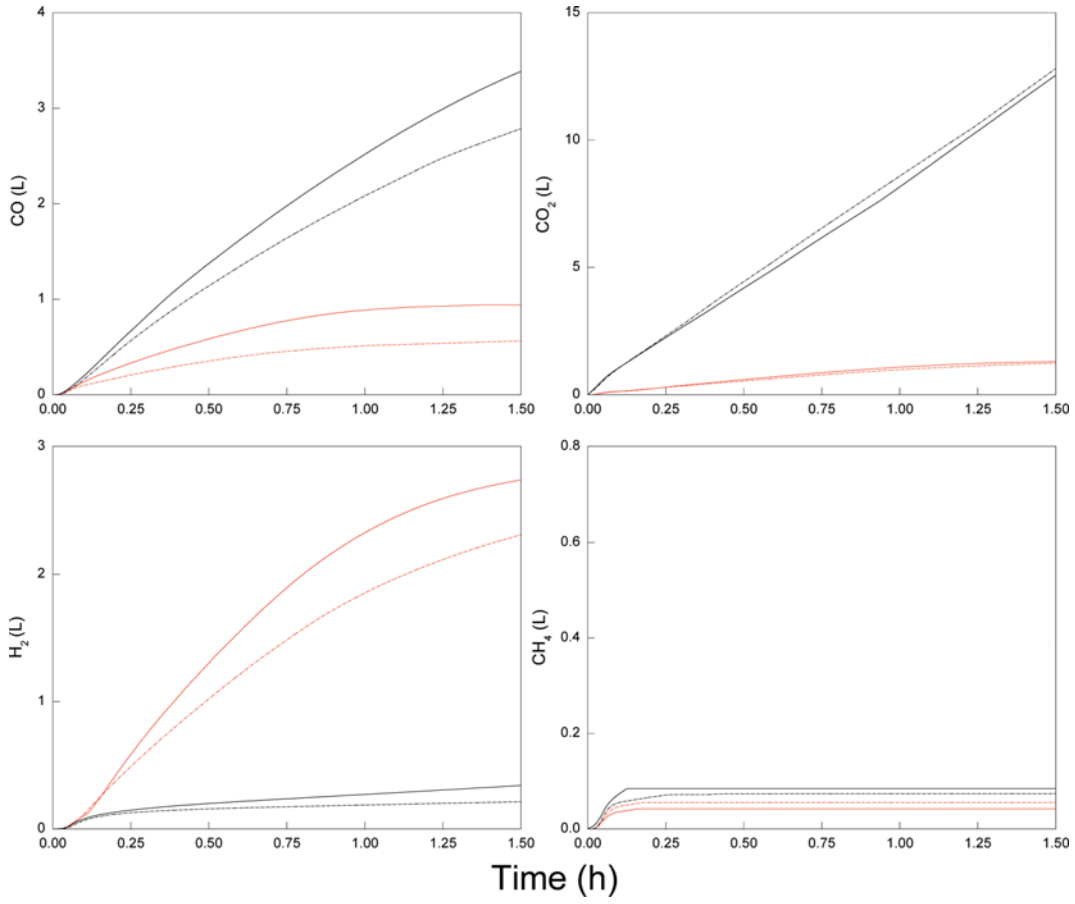

Fig. 5. Main products of coal gasification at 800 °C (red: using H_2O; black: using CO_2, Solid line: original coal; dotted line: pretreated coal).

The coal size decrement is an additional proof of the fact that bulk density of the coal was enhanced. Using the same fixed-bed reactor, more pretreated coal can be gasified. Besides, less ash means that less slag or fly ash might be dealt with.

2. FTIR Analysis Results

Inner structural changes were analyzed by FTIR. In Fig. 3, the FTIR spectra of the original ILRC (OILRC), pretreated ILRC (PILRC) and [Bmim]Cl show that PILRC shares no similar peaks with the characteristic absorptions of [Bmim]Cl at 1,573, 1,465 and 1,169 cm^{-1}, meaning that PILRC was thoroughly washed [15]. PILRC exhibits a notably higher absorbability compared to OILRC, meaning that part of the related bonds is destroyed by the ionic liquid and that bond polarity is increased [28].

The IL destroys cross-links in coal structure and dissolves some low molecular weight compounds. The chloride anion acts as a strong hydrogen bond acceptor, forming hydrogen bonds with various hydroxyl groups on the coal surface. These hydrogen bonds can replace inter and intramolecular hydrogen bonds in coal and lead to the dissolution of some low molecular weight compounds. Consequently, the active groups associated with that content decrease in number or weaken [28]. As shown in Table 1, the clear decrease of inner moisture and ash content proved that IL pretreatment can remove small molecules from coal and increase pore size.

Both pretreated and original coal exhibited aliphatic C-H stretches at around 2,920-2,850 cm^{-1} [28,29]. Pretreated coal showed a peak at 1,701 cm^{-1}, which was assigned to C=O bonds. The high content of the latter may be one reason for the higher production of CO_2, as it will be discussed in the gasification result part, in detail. Both coal samples also showed a peak at 1,577 cm^{-1}. Pretreated coal exhibited a wider range of aliphatic C-H bends compared to original coal, implying the presence of a greater number of C-H bonds. The higher C-H bond count may cause higher production of CH_4, especially in the steam-coal gasification, as shown in Figs. 4-6. Several peaks in the 1,300-1,100 cm^{-1} range [30] observed for original coal are attributable to phenoxy groups, while pretreated coal shows only one peak in this range, implying that a large proportion of phenoxy moieties is destroyed during the pretreatment and the structures are loosened. The bending vibration of methyl groups (1,376 cm^{-1}) in original coal samples contrasts with the strong C-O (1,170 cm^{-1}) stretch [31,32] of pretreated coal. The decrease of the number of C-O bonds during pyrolysis or gasification is controlled by diffusion [33]; after pretreatment, the pores are enlarged. A higher CO content is therefore possible, as shown in Fig. 6. Both pretreated and original coal displays out-of-plane vibration of aromatic C-H bonds at 818 cm^{-1} in the range of 900-700 cm^{-1} [29, 34]. Only pretreated coal has a detectable peak at 742 cm^{-1}, implying the presence of more than four CH_2 units in the chain.

3. BET Analysis Results

N_2 absorption analysis shows that the average pore diameter of pretreated coal (51.8 nm) is more than two-times larger than that

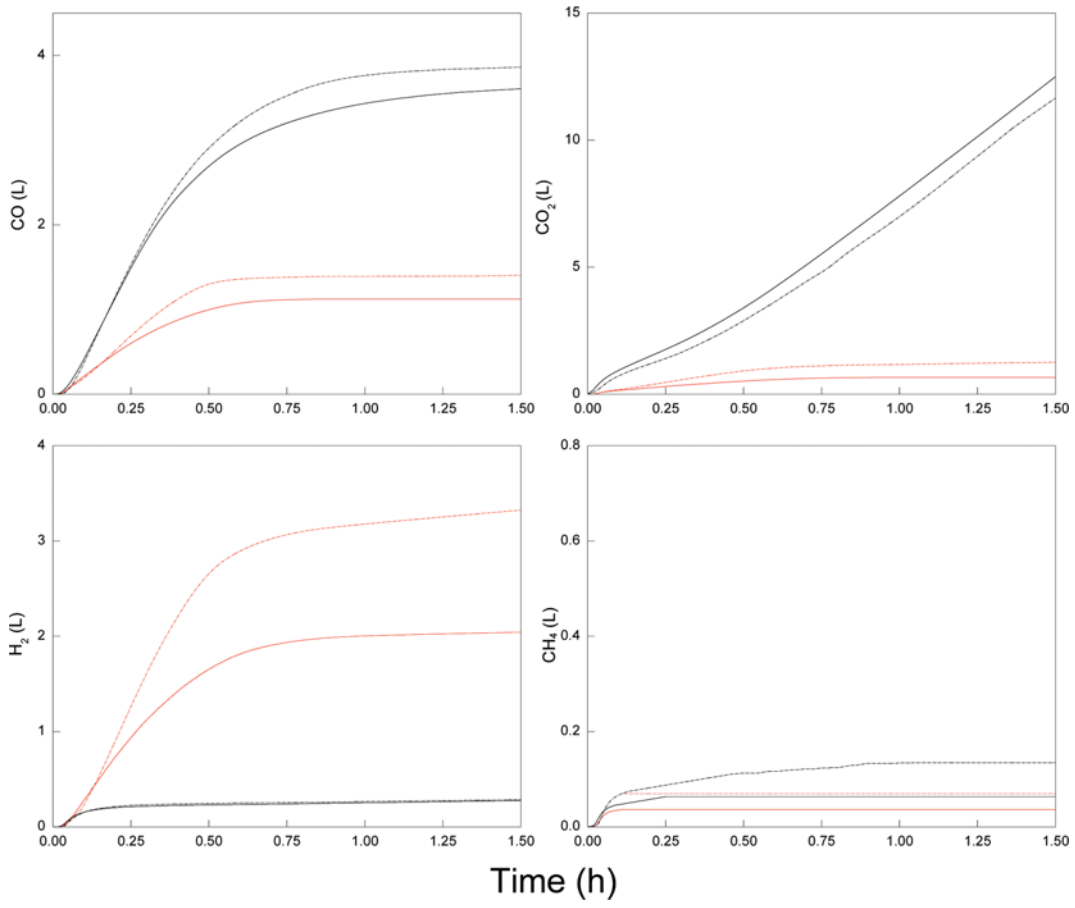

Fig. 6. Main products of coal gasification at 900 °C (red: using H_2O; black: using CO_2, Solid line: original coal; dotted line: pretreated coal).

Table 2. Comparison of pore characteristics of pretreated and original coal

Coal type	Solvent	Average pore diameter at desorption (nm)		Total pore volume at desorption (cm^3/g)		BET surface area (m^2/g)		Ref.
		Orig.	Pre.	Orig.	Pre.	Orig.	Pre.	
ILRC	[Bmim]Cl	23.6	51.8	0.019	0.009	2.275	0.218	-
CP No. 3 Anthracite	Tetrahydrofuran (THF)	9.75	9.76	0.0029	0.0040	0.8718	0.7144	[7]
YZ No. 5 Bituminous		14.4	13.96	0.0045	0.0074	0.5915	1.0171	
ZJ No. 9 Bituminous		8.55	17.73	0.0028	0.0359	0.4101	0.2089	
XG No. 8 Bituminous		4.65	7.76	0.0087	0.0111	4.6476	3.6706	
Springfield coal	CH_2Cl_2	5.7	6.7	0.02	0.01	16.9	6.5	[6]
	CH_3OH	5.7	5.9	0.02	0.02	16.9	12.5	
Lower block coal	CH_2Cl_2	4.4	4.5	0.06	0.03	62.9	36.1	
	CH_3OH	4.4	4.3	0.06	0.07	62.9	75.3	

of original coal (23.6 nm) (Table 2), while the total pore volume is lower than for original coal. Ji et al. [7] studied several coals extracted by ILs and found that in some cases mesopore volume increased by more than a factor of two, while the micropore volume did not change after extraction. The specific surface area decreased, while the average pore diameter increased after IL extraction. Furmann et al. [6] found that coal average volumes may increase or decrease, depending on the solvent used. The results of aforementioned previous researches ensure that the extractability of coal depends on solvent and coal rank. Pretreated coal volumes can be larger or smaller than the ones of the original, with pretreated coal pore diameter usually larger than for original coal.

BET equation was used to calculate the specific surface area in this work:

$$(P/P_0)/(V\times(1-P/P_0))=1/(V_m\times C)+(C-1)\times(P/P_0)/V_m \quad (10)$$

where P/P_0 denotes relative pressure, V is the volume of the adsorbed gas at P/P_0, V_m is the volume of the adsorbate monolayer

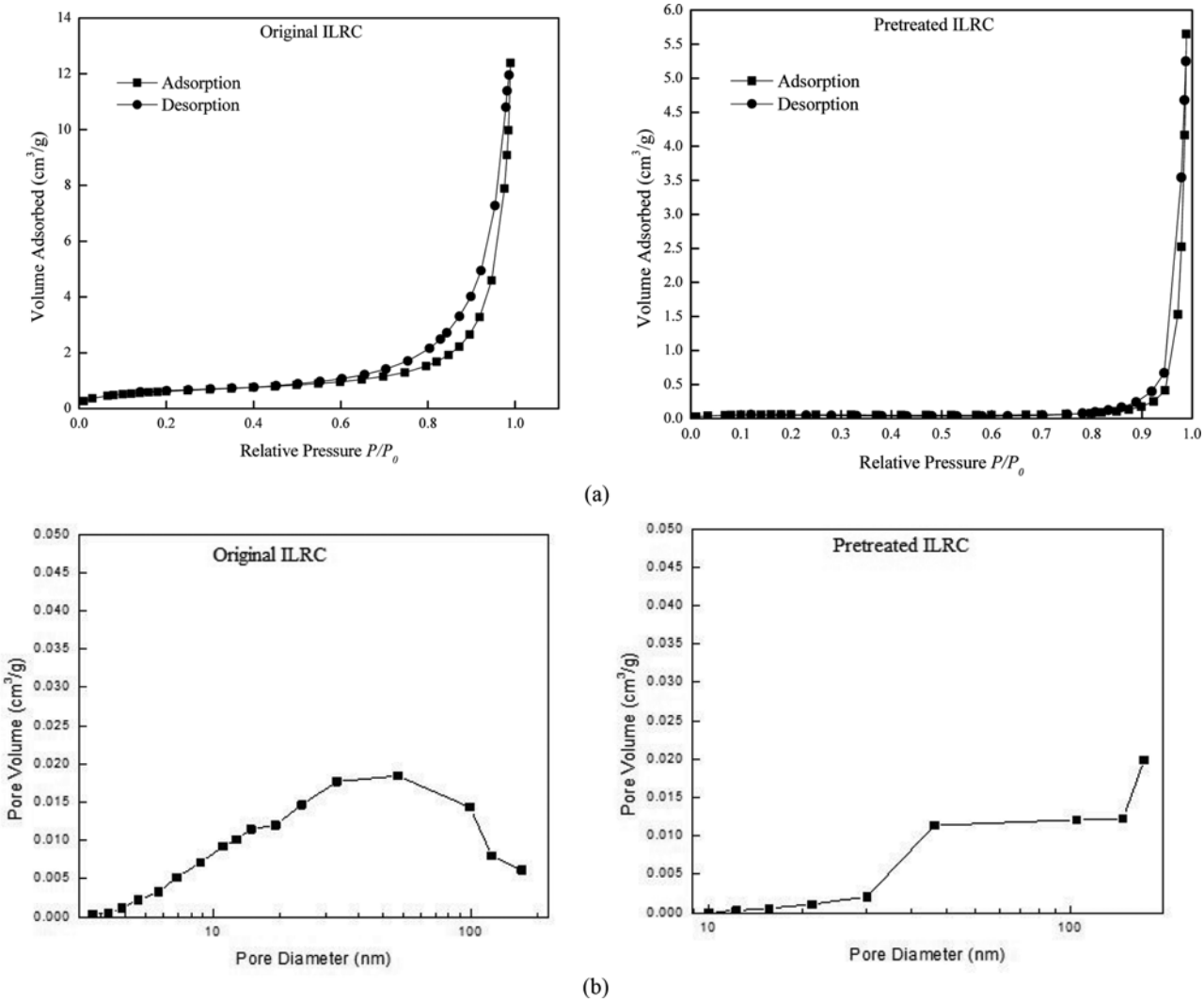

Fig. 7. BET analysis results of original and pretreated ILRC. (a) Isotherm plot of the volume adsorbed by original and pretreated ILRC as a function of pressure. (b) BJH desorption dV/dlog(D) of original and pretreated ILRC.

on the surface and C is the BET constant. Pretreated coal had a smaller BET surface area than original coal, as shown in Table 2.

Both pretreated and original coal exhibited high values of adsorbed volume during the desorption process. The difference indicated that pretreated coal had a smaller increase of the absorbed volume in the desorption than in the adsorption process. Besides, original coal showed higher volume absorbability than pretreated coal (Fig. 7(a)). The weight loss after extraction and the increase of pore diameter indicate that the IL pretreatment can not only expand the original holes (including macropores, mesopores and micropores), but also dissolve small molecules framed in the complicated coal matrix, and thus create a new pore structure.

The Barrett-Joyner-Halenda (BJH) theory was used to obtain meso- and macropore volumes and the average pore diameters. Fig. 7(b) shows that pores ranging from 1.7-300 nm had the biggest share of the total pore volume. The BJH desorption cumulative volume of pores with diameters between 1.7 and 300 nm was 0.009 cm^3/g for pretreated coal, whereas original coal had a much larger cumulative pore volume (0.019 cm^3/g). The desorption pore volume graph shows that the pore diameter of pretreated coal was mostly in the range of 40-100 nm, whereas the values for original coal were distributed in a wider range of 10-100 nm. This indicates an increase of the overall pore diameter and the predominance of macropores. Mesopores were dominant in original coal, with micropores having the least share. Resultingly, pretreatment with [Bmim]Cl increased coal pore diameter while decreasing the BET surface area and the total volume of pores with diameters between 1.7 and 300 nm.

4. Coal Gasification

To understand the IL pretreatment effect on coal gasification, both H_2O and CO_2 gasification were conducted. To obtain more exact values, three repetitive experiments were conducted for each gasification condition. The variance within each group of experiment results was smaller than 0.5%. The gas evolution trend and carbon conversion of pretreated coal were different with the values obtained from original coal. The main gas evolution trends are shown in Figs. 4-6. Carbon conversion was calculated according to Eq. (11):

$$X_c=(Vol_{CO}+Vol_{CO2}+Vol_{CH4})\times MWC/(N_a\times(T_{coal}\times F_c))\times 100 \quad (11)$$

where X_c is carbon conversion, Vol_{CO}, Vol_{CO2} and Vol_{CH4} indicate volumes of CO, CO_2 and CH_4, respectively, MWC is the molar weight of carbon, N_a is the volume of one mole of gas at standard conditions, T_{coal} is the total weight of input coal and F_c is the carbon content of coal.

The gasification results are in agreement with literature. Wang et al. [35] found that the IL-treated coal loses less weight than untreated coal before ignition, since most of the easily oxidized groups dissolve in ionic liquids and are washed away by distilled water during pretreatment. It was observed that the weight change rate of IL-treated coal was slower than that of the untreated coal during the whole process (<330 °C). At higher temperature, the increased weight loss rate indicates the activation of aromatic functional groups.

Figs. 4-6 show the main gas evolution trend as a function of time. At 700 and 800 °C, less CO gas was produced from pretreated coal than from original coal. It took the pretreated coal longer to convert completely. However, it showed obvious advantages over original coal at 900 °C. At lower temperature, gasification of pretreated coal was slower than of the original, possibly due to the loss of minerals during IL pretreatment. Researchers [36,37] found that alkali and alkaline earth metallic species (AAEM) catalyze char gasification. Calcite ($CaCO_3$) decomposed to CaO can simultaneously attract CO_2 and H_2O to the coal surface, making their reaction with coal much easier. Ca, Al and Si together constitute 60-80 wt% of ash in coal [38,39]. As described in Table 1, about 71.5% of ash was removed by IL pretreatment. The catalytic effect of Ca in gasification was greatly weakened for pretreated ILRC. As described in the FTIR part, more C=O bonds were present in pretreated than in original coal. The loss of ash as catalyst was offset by a higher C=O bond content. The CO_2 production in steam-coal and CO_2-coal gasification was almost the same at 700 and 800 °C. However, the enlarged coal pore size made gas diffusion easier at 900 °C and more CO_2 was generated in the steam-coal gasification. At high temperature (900 °C in this work), a reactivity enhancement was detected for both H_2O and CO_2 gasification, with the catalytic effect of ash weakening at higher temperature. The reaction rate was controlled by gas diffusion into pores (regime II). As described in the BET analysis part, the size of macro- and mesopores increased dramatically, with most of the micropores converted to mesopores. H_2O and CO_2 had easier access to micro- or mesopores via the enlarged macropores in pretreated coal. Therefore, at 900 °C, [Bmim]Cl pretreated coal showed obvious advantages over original coal in the gasification reaction.

Due to the introduction of CO_2 as gasification agent, it is difficult to calculate the carbon conversion for the CO_2 coal gasification. Only the carbon conversion of the steam-coal gasification at 900 °C was considered. Table 3 shows that pretreated coal had a carbon conversion of 97.25%, whereas original coal exhibited a value of 89.03%. More than 8% of coal was converted to syngas after pretreatment.

In the gasification temperature range (700-900 °C), steam-coal gasification generates about six times more hydrogen than CO_2 coal gasification. The hydrogen generated by the latter comes only from coal, while in the former, it also comes from steam.

Further analysis of coal gasification was conducted. Pretreated coal exhibited a larger slope increase of vol. (CO)/wt. (C) (L/g) than original coal in steam gasification, as shown in Fig. 8(a). The vol. (CO_2)/ wt. (C) (L/g) value for the gasification of original coal decreased at 900 °C, while pretreated coal exhibited a slight increase (Fig. 8(b)). The substantial CO_2 decrease may be due to the occurrence of the Boudouard reaction at the high temperature [40]. Origi-

Table 3. Carbon conversion (X_c) and CO_2 output comparison

	Orig. coal	Pre. coal
X_c[a] (900 °C)	89.03	97.25
CO_2/C (L/g)[b] (700 °C)	15.60	15.46
CO_2/C (L/g)[b] (800 °C)	13.29	13.41
CO_2/C (L/g)[b] (900 °C)	13.20	12.20

[a]H_2O was used as a gasification agent
[b]CO_2 was used as a gasification agent

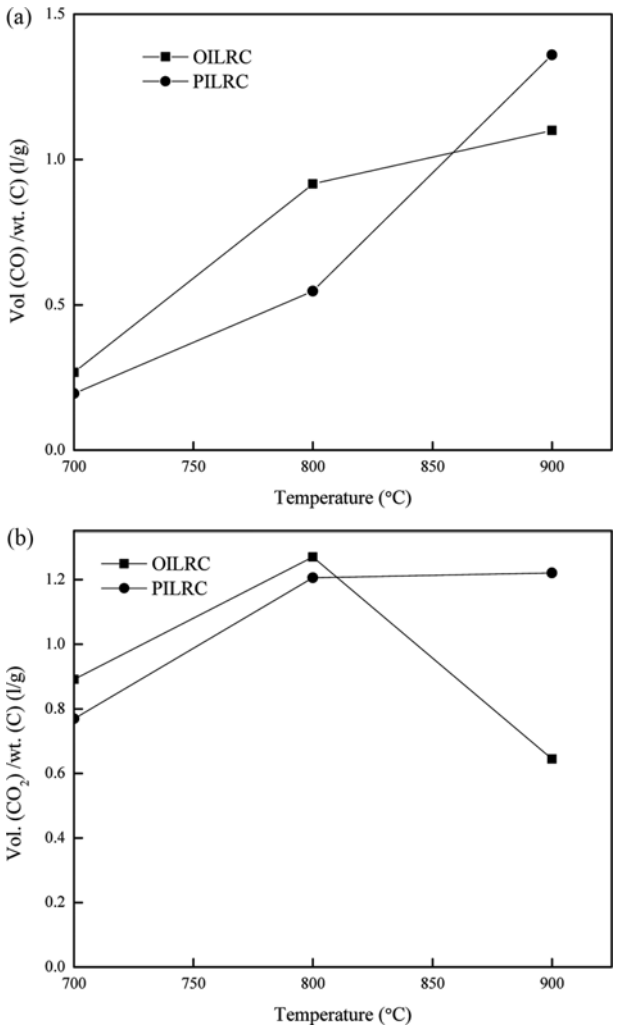

Fig. 8. Comparison of CO and CO_2 volume during steam-coal gasification (OILRC: original ILRC, PILRC: pretreated ILRC). (a) Output of vol. (CO)/wt. (C) (L/g) with H_2O as a gasification agent. (b) Output of vol. (CO_2)/wt. (C) (L/g) with H_2O as a gasification agent.

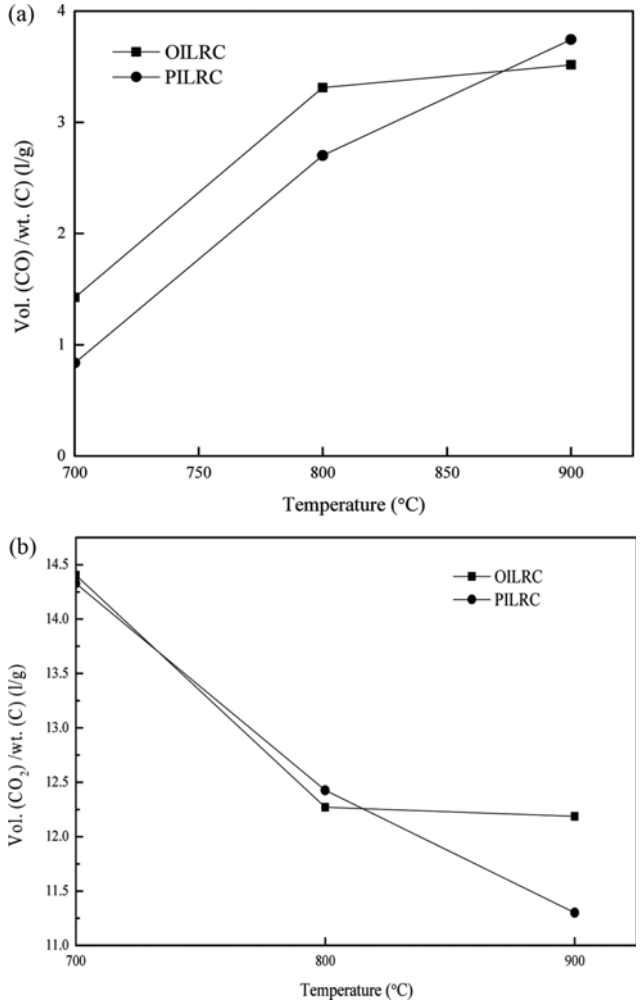

Fig. 9. Comparison of CO and CO_2 volume during CO_2 coal gasification (OILRC: original ILRC, PILRC: pretreated ILRC). (a) Output of vol. (CO)/wt. (C) (L/g) with CO_2 as a gasification agent. (b) Output of vol. (CO_2)/wt. (C) (L/g) with CO_2 as a gasification agent.

nal coal had a greater content of the catalytically active ash than pretreated coal. Pretreated coal provided better steam access to active sites, favoring reaction with solid carbon to generate H_2 and CO. As the syngas released from the active site and went from the coal, CO might have continuously reacted with steam, and thus the amount of CO_2 did not decrease, but slightly increased. The amount of generated hydrogen was greatly increased during steam-

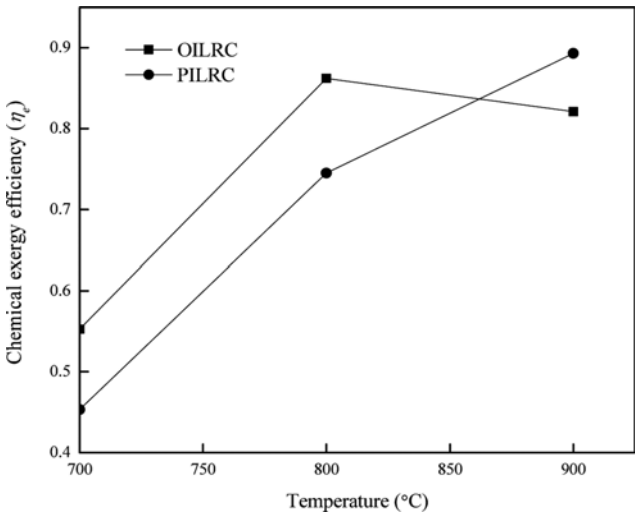

Fig. 10. Chemical exergy efficiency with CO_2 as a gasification agent (OILRC: original ILRC, PILRC: pretreated ILRC).

coal gasification, being 1.63-times of the amount produced from original coal at 900 °C (Fig. 6). The slope decrease of pretreated coal is smaller than that of original coal (Fig. 9(a)). More than 7 and 25% of CO were generated in pretreated coal gasification with CO_2 and H_2O, respectively (Fig. 6). Under the same conditions, pretreated coal gasification in CO_2 atmosphere reduced CO_2 emission by 6.7%, while pretreated coal gasification in H_2O atmosphere showed that almost two times more of CO_2 was generated. In the CO_2 gasification, at 900 °C, pretreated coal consumed large amounts of CO_2. CO_2 output volume per C gram of the pretreated coal gasification decreased sharply when the temperature was increased from 700 to 900 °C, as shown in Fig. 9(b). For every gram of C, gasification of pretreated coal resulted in the emission of one liter CO_2 less than the gasification of original coal at 900 °C. One liter of CO_2 contains about 0.53 g of C. This means that the original coal emitted 0.53 g more carbon as CO_2 for every gram of solid carbon during gasification. Therefore, [Bmim]Cl pretreatment has a great potential way to convert CO_2 into the useful fuel gas (CO) and consequently reduce CO_2 emission.

5. Exergy Analysis

The calculated chemical exergy, physical exergy of syngas, physical exergy of carrier gas, chemical exergy of coal and chemical exergy efficiency are listed in Table 4. The chemical exergy efficiency was calculated based on the total coal weight of 1.5 g.

Original coal had a much higher physical exergy than pretreated

Table 4. Exergy of syngas and feedstock and exergy efficiency

	Orig. 700 °C	Pre. 700 °C	Orig. 800 °C	Pre. 800 °C	Orig. 900 °C	Pre. 900 °C
E^{ch} (kJ/kg)	3977.11	3245.00	7847.51	6891.95	8933.71	9687.05
E^{ph} (kJ/kg)	361.76	361.98	454.14	451.51	545.52	523.51
$E^{ich}CO_2$ (kJ/kg)	451.49	451.49	451.49	451.49	451.49	451.49
$E^{iph}N_2$ & $E^{iph}CO_2$ (kJ/kg)	354.48	354.48	438.03	438.03	526.10	526.10
E_f^{ch} (MJ/kg-coal)	28.36	27.83	28.36	27.83	28.36	27.83
η_e	0.55	0.45	0.86	0.74	0.82	0.89

coal, as shown in Table 4, due to its lower content of oxygen and nitrogen. It is clear that both physical and chemical exergies of syngas increased as the gasification temperature was raised. Regarding chemical exergy, pretreated coal exhibited a lower value than that of original coal at 700 and 800 °C, but a higher value at 900 °C. The chemical exergy efficiency of syngas to input feedstock increased with increasing temperature. The chemical exergy efficiency of pretreated coal was higher than that of original coal at 900 °C (Fig. 10).

All of the above results indicate that pretreated coal generates syngas with a higher chemical exergy efficiency at 900 °C. Pretreatment is favorable at higher gasification temperature, being not only able to increase chemical exergy efficiency, but also reduce CO_2 emission.

CONCLUSIONS

The pretreatment effect of coal by ionic liquid and its own properties and gasification characteristic were investigated. The structure of coal pretreated with [Bmim]Cl was dramatically changed. Most of the small, easily volatilized molecules and ash were dissolved and washed away during pretreatment and subsequently washed with distilled water. The loss of small molecules and catalytic ash reduced the gasification rate, especially at low temperature (700 and 800 °C).

However, at high temperatures (in particular, 900 °C in this work), when the reaction rate was governed by gas diffusion, the pretreated coal indicated a clearly higher gasification rate due to the larger pore size (more than two times compared to original coal). Pretreated coal generated 1.63-times the amount of hydrogen compared to original coal in steam-coal gasification at 900 °C. When CO_2 was used as gasification agent, pretreated coal consumed much more CO_2 and generated more CO than original coal. For every gram of coal, original coal gasification with CO_2 led to the emission of one liter of CO_2 more than pretreated coal. Coal pretreatment with [Bmim]Cl enhanced the consumption of CO_2, resulting in higher purity CO production than that under steam-coal gasification.

The carbon conversion of coal by pretreatment increased from 89.03% to 97.25% during steam-coal gasification. The chemical exergy of pretreated coal was lower than that of the original coal due to its higher content of oxygen and nitrogen. Syngas from pretreated coal had higher chemical exergy than original coal under CO_2 gasification condition. The chemical exergy efficiency of pretreated coal increased to 7% in comparison with original coal at 900 °C.

ACKNOWLEDGEMENTS

This work was supported by the Human Resources Program in Energy Technology of the Korea Institute of Energy Technology Evaluation and Planning (KETEP). Financial support was granted by the Ministry of Trade, Industry & Energy, Republic of Korea. (Project No. 2015 4010 200820).

NOMENCLATURE

E^{ch} : chemical exergy of gaseous components [kJ/kg]
$E^{ich}CO_2$: chemical exergy of input CO_2 [kJ/kg]
$E^{ch}el^0$: standard (298.15 K, 101.325 kPa) chemical exergy of elements [kJ/mol]
E_f^{ch} : chemical exergy of coal [MJ/kg]
$E^{ch}S$: chemical exergy of syngas [kJ/kg]
E^{ph} : physical exergy of a pure substance [kJ/kg]
$E^{iph}CO_2$: physical exergy of input CO_2 from room temperature to predetermined gasification temperature [kJ/kg]
$E^{iph}N_2$: physical exergy of input N_2 from room temperature to predetermined gasification temperature [kJ/kg]
$E^{ph}S$: physical exergy of syngas [kJ/kg]
H : enthalpy at given temperature and pressure [kJ/kg]
H_c : enthalpy at standard temperature and pressure (298.15 K and 1 atm) [kJ/kg]
HHV_s : high heating value of syngas [MJ/kg]
HHV_f : high heating value of coal [MJ/kg]
H_{orig} : height of original coal [cm]
H_{pre} : height of pretreated coal [cm]
m_s : mass flow rate of syngas [kg/h]
m_f : mass flow rate of fuels [kg/h]
MWC : molar weight of carbon [g/mol]
N_a : volume of one mole of gas at standard conditions [L/mol]
n_{el} : number of moles of elements [mol]
n(C) : mole fraction of carbon
n(H) : mole fraction of hydrogen
n(O) : mole fraction of oxygen
OILRC : original ILRC
PILRC : pretreated ILRC
Orig. : original
Pre. : pretreatment
P/P_0 : relative pressure
Q : swelling ratio
S : entropy at given temperature and pressure [kJ/kg]
S_0 : entropy at 298.15 K and 1 atm [kJ/kg]
T_0 : standard temperature of 298.15 K
T_{coal} : total weight of input coal [g]
V : volume of the adsorbed gas at P/P_0 [cm^3]
V_m : volume of adsorbate monolayer on the surface [cm^3]
Vol_{CH4} : volume of CH_4 (L)
Vol_{CO} : volume of CO (L)
Vol_{CO2} : volume of CO_2 (L)
X_c : carbon conversion
Z_A : weight fraction of ash [wt% dry]
Z_C : weight fraction of carbon [wt% dry]
Z_H : weight fraction of hydrogen [wt% dry]
Z_N : weight fraction of nitrogen [wt% dry]
Z_O : weight fraction of oxygen [wt% dry]
Z_S : weight fraction of sulfur [wt% dry]
β : correlation value of chemical exergy of coal
$\Delta_f G^0$: standard gibbs free energy of formation [kJ/kg]
η_c : cold gas efficiency
η_e : exergy efficiency

REFERENCES

1. T. J. Kang, H. J. Park, H. Namkung, L. H. Xu, S. Fan and H. T.

Kim, *Korean J. Chem. Eng.*, **34**, 1238 (2017).
2. S. H. Kang, S. J. Lee, W. H. Jung, S. W. Chung, Y. Yun, S. H. Jo, Y. C. Park and J. I. Baek, *Korean J. Chem. Eng.*, **30**, 67 (2013).
3. J. Lee, S. H. Kang, H. S. Kim, D. H. Jeon, S. J. Lee, S. W. Chung, J. W. Lee, Y. Yun, H. J. Ryu and J. I. Baek, *Korean J. Chem. Eng.*, **33**, 2610 (2016).
4. T. J. Kang, H. J. Park. H. Namkung, L. H. Xu, J. H. Park, I. Heo, T. S. Chang, B. S. Kim and H. T. Kim, *Korean J. Chem. Eng.*, **34**, 2597 (2017).
5. E. Komarova, S. Guhl and B. Meyer, *Fuel*, **152**, 38 (2015).
6. A. Furmann, M. Mastalerz, S. C. Brassell, A. Schimmelmann and F. Picardal, *Int. J. Coal. Geol.*, **107**, 141 (2013).
7. H. Ji, Z. Li, Y. Peng, Y. Yang, Y. Tang and Z. Liu, *J. Nat. Gas Sci. Eng.*, **19**, 287 (2014).
8. C. R. Clarkson and R. M. Bustin, *Fuel*, **78**, 1333 (1999).
9. M. Zou, C. Wei, Z. Huang and S. Wei, *J. Nat. Gas Sci. Eng.*, **27**, 776 (2015).
10. G. N. Okolo, R. C. Everson, H. W. J. P. Neomagus, M. J. Roberts and R. Sakurovs, *Fuel*, **141**, 293 (2015).
11. J. Tanner and S. Bhattacharya, *Chem. Eng. J.*, **285**, 331 (2016).
12. L. Y. Wang, S. G. Jiang, Y. L. Xu, W. Q. Zhang, L. W. Kou, Z. Y. Wu and T. X. Chu, *Procedia Eng.*, **26**, 647 (2011).
13. X. Fan, X. Y. Wei and Z. M. Zong, *Fuel*, **109**, 28 (2013).
14. Z. P. Lei, L. L. Cheng, S. F. Zhang, Y. Q. Zhang, H. F. Shui, S. B. Ren and Z. C. Wang, *Fuel Process. Technol.*, **129**, 222 (2015).
15. S. Liu, W. Zhou, F. Tang, B. Guo, Y. Zhang and R. Yin, *Fuel*, **160**, 495 (2015).
16. S. Fan, X. Yuan, L. Zhao, L. H. Xu, T. J. Kang and H. T. Kim, *Fuel*, **165**, 397 (2016).
17. Z. Lei, L. Wu, Y. Zhang, H. Shui, Z. Wang and S. Ren, *Fuel Process. Technol.*, **111**, 118 (2013).
18. R. Cetiner [Dissertation], *Fragmentation of coal and improved dispersion of liquefaction catalysts using ionic liquids*, The Pennsylvania State University (2011).
19. Z. Lei, L. Wu, Y. Zhang, H. Shui, Z. Wang, C. Pan, H. Li, S. Ren and S. Kang, *Fuel*, **95**, 630 (2012).
20. J. Cummings, K. Shah, R. Atkin and B. Moghtaderi, *Fuel*, **143**, 244 (2015).
21. M. J. Prins, K. J. Ptasinski and F. J. Janssen, *Energy*, **32**, 1248 (2007).
22. M. Juraščík, A. Sues and K. J. Ptasinski, *Energy*, **35**, 880 (2010).
23. R. Karamarkovic and V. Karamarkovic, *Energy*, **35**, 537 (2010).
24. I. Janajreh, S. S. Raza and A. S. Valmundsson, *Energy Convers. Manage.*, **65**, 801 (2013).
25. C. He, X. Feng and K. H. Chu, *Appl. Energy*, **111**, 742 (2013).
26. S. Channiwala and P. Parikh, *Fuel*, **81**, 1051 (2002).
27. J. Szargut, D. R. Morris and F. R. Steward, *Exergy analysis of thermal, chemical, and metallurgical processes*, Hemisphere, New York (1987).
28. W. Zhang, S. Jiang, Z. Wu and H. Shao, *Int. J. Min. Sci. Technol.*, **22**, 687 (2012).
29. J. Ibarra, E. Munoz and R. Moliner, *Org. Geochem.*, **24**, 725 (1996).
30. L. Zhang, S. Kajitani, S. Umemoto, S. Wang, D. Quyn, Y. Song, T. Li, S. Zhang, L. Dong and C. Z. Li, *Fuel*, **158**, 711 (2015).
31. Z. Wang, L. Li, H. Shui, Z. Lei, S. Ren, S. Kang and C. Pan, *J. Fuel Chem. Technol.*, **39**, 401 (2011).
32. M. Guillen, M. Iglesias, A. Dominguez and C. Blanco, *Energy Fuels*, **6**, 518 (1992).
33. Z. Niu, G. Liu, H. Yin, D. Wu and C. Zhou, *Fuel*, **172**, 1 (2016).
34. L. Bai, Y. Nie, J. Huang, Y. Li, H. Dong and X. Zhang, *Fuel*, **112**, 289 (2013).
35. L. Wang, Y. Xu, S. Jiang, M. Yu, T. Chu, W. Zhang, Z. Wu and L. Kou, *Saf. Sci.*, **50**, 1528 (2012).
36. B. B. Hattingh, R. C. Everson, H. W. Neomagus and J. R. Bunt, *Fuel Process. Technol.*, **92**, 2048 (2011).
37. Y. L. Wang, S. H. Zhu, M. Q. Gao, Z. R. Yang, L. J. Yan, Y. H. Bai and F. Li, *Fuel Process. Technol.*, **141**, 9 (2016).
38. G. Skodras and G. Sakellaropoulos, *Fuel Process. Technol.*, **77**, 151 (2002).
39. C. Thiel, M. Pohl, S. Grahl and M. Beckmann, *Fuel*, **152**, 88 (2015).
40. C. G. Lee and H. Hur, *Korean J. Chem. Eng.*, **28**, 1539 (2011).